



Simultaneous determination of Aprepitant and two metabolites in human plasma by high-performance liquid chromatography with tandem mass spectrometric detection

C.M. Chavez-Eng*, M.L. Constanzer, B.K. Matuszewski

Merck & Co. Inc., WP42-208, Merck Research Laboratories, P.O. Box 4, West Point, PA 19486, USA

Received 20 February 2004; received in revised form 26 March 2004; accepted 29 March 2004

Available online 5 June 2004

Abstract

A method for the simultaneous determination of Aprepitant, **I** (5-[[2(R)-[1(R)-(3,5-bistrifluoromethylphenyl)ethoxy]-3(S)-(4-fluorophenyl) morpholin-4-yl]methyl]-2,4-dihydro-[1,2,4]triazol-3-one) and two active metabolites (**II** and **III**) in human plasma has been developed. The method was based on high-performance liquid chromatography (HPLC) with atmospheric pressure chemical ionization tandem mass spectrometric (APCI-MS-MS) detection in positive ionization mode using a heated nebulizer interface. The analytes and internal standard (**IV**) (Fig. 1) were isolated from basified plasma using liquid–liquid extraction. The organic extracts were dried, reconstituted in mobile phase and injected into the HPLC-MS/MS system.

The analytes were chromatographed on a narrow bore (50 mm × 2.0 mm, 3 μm) Keystone Scientific's Prism R.P. analytical column, with mobile phase consisting of acetonitrile (ACN):water containing trifluoroacetic acid with pH adjusted to 3 (40:60, v/v) pumped at a flow rate of 0.5 ml/min. The MS-MS detection was performed on a Sciex API 3000 tandem mass spectrometer operated in selected reaction monitoring mode. The precursor → product ion combinations of m/z 535 → 277, 438 → 180, 452 → 223 and 503 → 259 were used to quantify **I**, **II**, **III**, and **IV**, respectively, after chromatographic separation of the analytes. The assay was validated in the concentration range of 10–5000 ng/ml for **I** and **II** and 25–5000 ng/ml for **III** when 1 ml of plasma was processed. The precision of the assay (expressed as coefficient of variation, CV) was less than 10% at all concentrations within the standard curve range, with adequate assay accuracy. Matrix effect experiments were performed to demonstrate the absence of any significant change in ionization of the analytes when comparing neat standards to analytes in the presence of plasma matrix. This assay was utilized to support a clinical study where multiple oral doses of **I** were administered to healthy subjects to investigate the pharmacokinetics, safety, and tolerability of Aprepitant. Concentrations of the two most active metabolites, which if present in high concentrations would increase the neurokinin-1 (NK₁) receptor occupancy level and therefore potentially contribute to the antiemetic action of Aprepitant, were determined.

© 2004 Elsevier B.V. All rights reserved.

Keywords: Aprepitant; Plasma; High-performance liquid chromatography

* Corresponding author. Tel.: +1-215-652-4711; fax: +1-215-652-8548.
E-mail address: cynthia_chavezeng@merck.com (C.M. Chavez-Eng).

1. Introduction

Aprepitant, **I** (2*R*)-[1(*R*)-(3,5-bis-trifluoromethyl-phenyl)ethoxy]-3(*S*)-(4-fluoro-phenyl)morpholin-4-ylmethyl]-5-oxo-(4,5-dihydro-[1,2,4] triazol) methyl morpholine (Fig. 1), a potent and selective, brain-penetrant neurokinin-1 (NK₁) receptor antagonist, has been demonstrated to be effective in the prevention of chemotherapy-induced nausea and vomiting (CINV) [1–4]. **I** was highly effective in the control of emesis thereby reducing the impact of CINV on cisplatin-treated patients' daily lives [5].

Metabolism of Aprepitant has been studied in rats [6], dogs [6], and in ferrets [7]. The two most pharmacologically active metabolites of **I** are **II** and **III** and were found, although in relatively minor amounts, in the plasma samples and brain extracts of ferrets 48 h after dosing with **I** suggesting that these two metabo-

lites are the most brain penetrating [7]. It was reported that the in vitro binding affinities (IC₅₀) of the metabolites to the human NK₁ receptor have a much reduced binding affinity (0.5 nM for **II**; 1.7 nM for **III**) when compared with Aprepitant (0.12 nM). Based on this study, it was hypothesized that Aprepitant is responsible for the antiemetic activity in humans.

As brain penetration and subsequent receptor occupancy are important factors contributing to the effect of Aprepitant in the CIE response, an assessment of the concentrations of these two active metabolites in plasma samples from a clinical study may help in determining whether the antiemetic activity is inherent with Aprepitant or with its metabolites or both.

In humans, the adsorption, metabolism and excretion of Aprepitant following a single IV and oral administration of ¹⁴C-labeled prodrug of Aprepitant and ¹⁴C-Aprepitant has been reported [8]. It

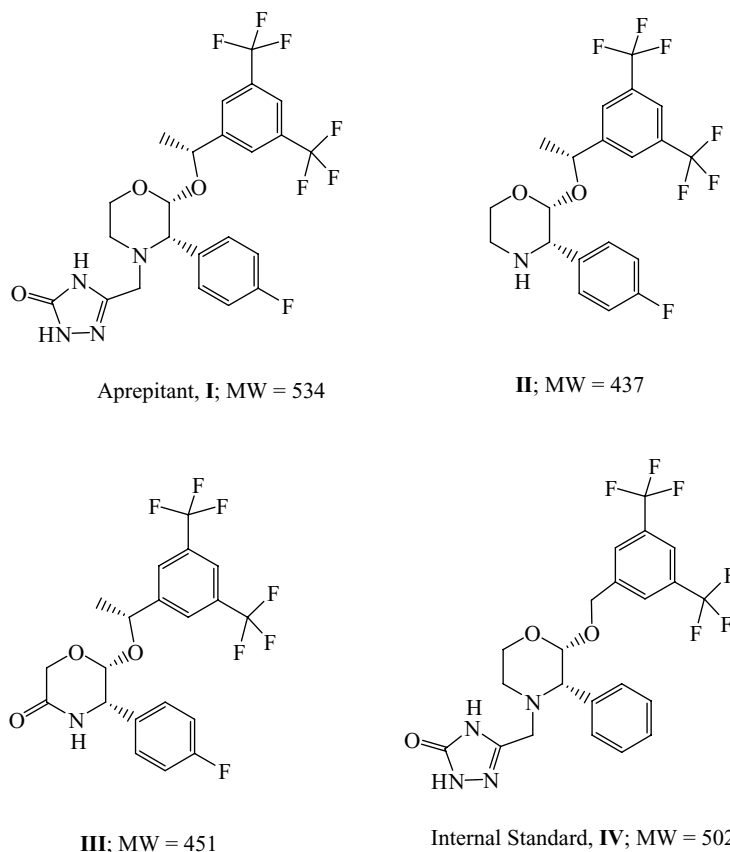


Fig. 1. Chemical structures of Aprepitant (**I**), metabolites (**II** and **III**), and internal standard (**IV**).

was found that the major metabolic pathways of Aprepitant including *N*-dealkylation, oxidation and morpholine ring-opening, *O*-dealkylation, triazolone ring-opening and glucuronidation were similar among rats, dogs, and humans. Qualitative identification and confirmation analyses of these metabolites were performed utilizing HPLC-MS/MS [8] and HPLC-NMR [9] techniques. For the clinical evaluation of **I**, bioanalytical methods for the determination of **I** in human plasma and urine based on high-performance chromatography (HPLC) with atmospheric-pressure chemical ionization (APCI) mass spectrometric (MS) detection using either single (MS) or triple (MS/MS) quadrupole mass spectrometric detection have been reported by us earlier [10]. However, when applied to the simultaneous determination of **I**, **II**, and **III**, this method was inadequate due to the lack of selectivity and the potential presence of matrix effect due to co-elution of analytes (**I** and **II**) that were quantified. Therefore, the chromatographic conditions were modified to eliminate the matrix effects and experiments confirming assay selectivity and the absence of matrix effect for all three analytes determined simultaneously were performed.

The described experiments may serve as a general example of how methods for multiple analytes are to be validated and how the absence of matrix effect for all analytes may be demonstrated. The subject of this paper is the development of the bioanalytical method for the simultaneous determination of **I**, and metabolites **II** and **III** in human plasma. The method was used for supporting a clinical study with **I** in which concentrations of all three compounds **I**, **II**, and **III** were determined simultaneously in the same analytical run.

2. Experimental

2.1. Materials

Compounds **I**, **II**, **III**, and **IV** (Fig. 1) with purity of greater than 99 % were received from the Merck Research Laboratories (Rahway, NJ) sample repository. All solvents, namely, methanol (99.9%), acetonitrile (ACN) (99.9%), methyl *t*-butyl ether (MTBE, 99.9%), were purchased from Fisher Scientific (Fair Lawn, NJ). Trifluoroacetic acid (98.6%) and ammonium acetate (99.1%) were also purchased from Fisher Sci-

entific. The different lots of drug-free EDTA treated plasma originated from Biological Specialty (Lansdale, PA). Liquid Nitrogen (99.999%) was purchased from West Point Supply (West Point, PA).

2.2. Instrumental

A Sciex (Thornhill, Canada) API 3000 tandem mass spectrometer equipped with a heated nebulizer (HN) interface, a PE 200 autoinjector, and a PE 200 Quaternary pump were used for all analyses. The data were processed using MacQuan software (Sciex) on an IBM PC compatible computer.

2.3. Standard solutions

Stock standard solutions (100 µg/ml) for **I**, **II**, **III**, and **IV** were prepared in methanol. The stock solutions of **I**, **II**, and **III** were further diluted with methanol to give a series of working standards of 0.1 to 50 µg/ml. The internal standard (**III**) stock solution (100 µg/ml) in methanol was serially diluted with methanol to yield a working standard of 2.5 µg/ml.

2.4. Chromatographic conditions

Chromatographic separation of analytes was performed on a Keystone Scientific's Prism R.P. analytical column (50 mm × 2 mm, 3 µm particle size, Keystone Scientific, Bellefonte, PA) and a mobile phase consisting of 40% acetonitrile and 60% water containing trifluoroacetic acid, TFA (0.1%) with pH adjusted to 3, pumped at a flow rate of 0.5 ml/min. The total runtime was 9 min. All analytes were baseline separated. The retention times of **I**, **II**, **III**, and **IV** were 4.2, 1.0, 6.8, and 3.2 min corresponding to capacity factors (*k'*) of 20, 4, 33, and 15, respectively.

2.5. HPLC-mass spectrometric detections conditions

A Sciex (API 3000) triple quadrupole mass spectrometer was interfaced via a Sciex HN probe with the HPLC system. The HN probe was maintained at 500 °C and gas phase chemical ionization was effected by a corona discharge needle (+4 µA) using positive ion atmospheric pressure chemical ionization (APCI). The nebulizing gas (N₂) pressure was set for the HN interface at 80 psi. The curtain gas flow (N₂) was at a

setting of 12, and the sampling orifice potential was +35 V. The mass analyzers were operated at unit mass resolution. The mass spectrometer was programmed to admit the protonated molecules $[M + H]^+$ at m/z 535, 438, 452, and 503 for **I**, **II**, **III**, and **IV**, respectively, via the first quadrupole filter (Q1). Collision induced fragmentation at Q2 (CAD gas setting of 4) yielded the product ions at m/z 277, 180, 223, and 259 for **I**, **II**, **III**, and **IV**, respectively, and were detected at Q3. Peak area ratios (analytes versus internal standard) obtained from multiple reaction monitoring (MRM) of the analytes were utilized for the construction of calibration curves. Weighted ($1/x^2$) linear least-square regression of the plasma concentrations and measured peak area ratios were used for the quantification of the three analytes. Data collection, peak integration and calculations were performed using RAD and MacQuan Sciex software.

2.6. Sample preparation

Seven different standard curves in mobile phase and human plasma were constructed to evaluate the assay accuracy, precision, recovery, and the absence or presence of the matrix effect. The first standard curve (Curve 1) was constructed to evaluate the MS/MS response for neat standards of all 4 analytes injected in the mobile phase. The second curve (Curve 2) was constructed in plasma extracts originating from a single lot of plasma to which analytes were spiked *after* extraction. In addition, a set of samples corresponding to five standard curves (Set 1, Curves A–E; 8 concentrations \times 5 = 40 samples) was prepared in plasma from five different lots. The plasma samples in this set were spiked with standards *before* extraction. The first curve of this set was constructed in the same plasma lot as used during the construction of Curve 2. By comparing the absolute peak areas of the analytes, the peak areas ratios, and slopes of the standard curves from Curves 1, 2, and standard curves constructed in five different plasma lots, the absence or presence of matrix effect [11,12], precision and accuracy of the method, and recovery of the analytes were assessed.

The samples were prepared in the following manner:

Curve 1—A standard curve of neat standards at 8 concentrations was constructed by placing 100 μ l of the appropriate standard mixture of **I**, **II**, and **III**,

and 100 μ l of IS (**IV**), both in methanol, into 15 ml centrifuge tubes containing 800 μ l of mobile phase. The solution was vortexed then transferred to the autosampler vial, and 10 μ l was injected into the HPLC-MS/MS system.

Curve 2—A standard curve at 8 concentrations was constructed in one lot of plasma by adding 1 ml of plasma to a 15 ml centrifuge tube followed by the addition of 200 μ l of methanol. The plasma was basified with pH 9.8 carbonate buffer (1 ml) and extracted with 7 ml MTBE. The mixture was centrifuged (2060 \times g) for 5 min to separate the layers, then the tubes were placed in a dry ice/acetone bath to freeze the aqueous layer. The entire organic layer was decanted to a clean tube and evaporated to dryness under a stream of nitrogen in a 50 °C water bath. The residue was dissolved in 800 μ l of mobile phase to which 100 μ l of the appropriate standard mixture of **I**, **II**, and **III**; and IS (100 μ l), both in methanol, was added. The solution was vortexed, transferred to the autosampler vial, and 10 μ l was injected into the HPLC-MS/MS systems.

Set 1—Standard curves (A–E) at 8 concentrations were constructed in plasma from five different sources. Standard curve A of this set was constructed in the same plasma lot as the one used for the construction of Curve 2 (analytes spiked after extraction). One ml of plasma was placed in a 15 ml centrifuge tube to which 100 μ l each of appropriate standard mixture of **I**, **II**, and **III** and 100 μ l of IS (**IV**), both in methanol, were added. The control (blank) tubes had 1 ml of plasma to which 200 μ l of methanol was added. Mixtures placed in the tubes were basified by adding 1 ml of pH 9.8 carbonate buffer and analytes were extracted with 7 ml of MTBE. The organic layer was separated and evaporated to dryness following the same procedures as performed in preparing the dried extracts for Curve 2. The residue was dissolved in 800 μ l of mobile phase (40/60 mixture of acetonitrile/water containing 0.1% TFA adjusted to pH 3.0 with ammonium hydroxide) to which an additional 200 μ l of methanol was added. Ten microliters of these extracts was injected into the HPLC-MS/MS systems.

2.7. Precision, accuracy, and recovery

The precision of the method was determined by the replicate analyses ($n = 5$, set 1) of **I**, **II**, and

III in five different sources of human plasma at all concentrations utilized for the construction of calibration curves. The linearity of each standard curve was confirmed by plotting the peak area ratio of each analyte to IS (**IV**) versus analyte concentration. The unknown sample concentrations were calculated from the equation $y = mx + b$, as determined by weighted ($1/x^2$) linear regression of each standard curve. The accuracy of the method was expressed by [(mean observed concentration)/(spiked concentration)] \times 100 (set 1). The recovery was determined by comparing the mean peak areas of **I**, **II**, or **III** in set 1 to those observed during the construction of Curve 2.

2.8. Assessment of the matrix effect

The matrix effect and assay reliability for all three analytes **I**, **II**, and **III** was assessed in a similar manner as described previously for a single analyte [11,12] by comparing the peak areas of all analytes in different lots of plasma, the peak area ratios of analytes to an internal standard, and by analyzing plasma samples spiked before and after extraction. In addition, the recovery of the extraction procedure and the absolute matrix effect (ion suppression or enhancement) were assessed for all three analytes.

2.9. Assessment of assay selectivity

The assay selectivity was assessed by analyzing extracts from five lots of plasma originating from different sources. Endogenous peaks at the retention times of the analytes of interest were not observed in any of the plasma lots evaluated. In addition, the “cross-talk” between the MS/MS channels monitored for the analytes and **IS** was evaluated by injecting separately each analyte at the highest concentration on the standard curve and monitoring the responses in all other MS/MS channels.

2.10. Clinical sample preparation

The clinical study samples were originally analyzed for the concentration of the parent drug, **I** using 1 ml of plasma. Due to the limited volume of plasma remaining, it was not feasible to reassay all the samples from the study for metabolite concentrations

using 1 ml of plasma. Therefore, plasma samples from selected subjects at the same time points were pooled and then assayed for **I**, **II**, and **III** concentrations. Four subjects each from the male and female panels who received 125 mg dose of **I** were selected to be pooled based on their high **I** concentrations during the initial assay. The male and female panels were independently pooled in order to examine any potential differences in the metabolism between the sexes. The samples were pooled by removing a 0.5 ml aliquot from a given subject time-point sample and combining it with similar aliquots from other subjects at the same time point. This was repeated at all other time points for the same subjects resulting in the entire time profile from two parts of the study. These aliquots were mixed and frozen at -20°C .

The liquid–liquid extraction method consisted of adding base (pH 9.8 carbonate buffer, 1 ml), to 1 ml of plasma, spiked with 100 μl of internal standard solution (2.5 $\mu\text{g}/\text{ml}$) and then extraction with methyl-*t*-butyl ether (7 ml) in conical disposable glass tubes (15 ml) by rotating mixing. The organic extract was transferred to a clean 15 ml centrifuge tube and evaporated under a stream of nitrogen at 50°C . The dried residue was reconstituted in mobile phase (1 ml) and 10 μl of this solution was injected into the HPLC system.

2.11. Quality control sample preparation

Quality control (QC) samples at three different concentrations were prepared from a pool of five different lots of plasma. Five hundred microliter each of a 400, 150, and 10 $\mu\text{g}/\text{ml}$ standard solution in methanol of **I**, **II**, and **III** (prepared from a new weighing) was pipetted into a 50 ml volumetric flask, to prepare the high (4000 ng/ml), medium (1500 ng/ml), and low (100 ng/ml) QCs, respectively. Each flask was q.s. to the mark with control plasma and vortexed for 30 s.

The quality control solutions at each concentration were then aliquotted (1.25 ml) into polypropylene tubes and the tubes were kept frozen at -20°C .

2.12. Quality control freeze–thaw stability

Quality control samples were examined for their freeze–thaw stability. Freshly prepared QC samples

were frozen for at least 24 h and thawed unassisted at room temperature. After thawing, the samples were refrozen for at least 12 h then thawed a second time. This freeze–thaw cycle was repeated, and then samples were analyzed after completing the third freeze–thaw cycle.

3. Results and discussion

3.1. Method validation

Full scan positive ion mass spectra of **I**, **II**, **III**, and **IV** yielded predominantly the protonated molecules at

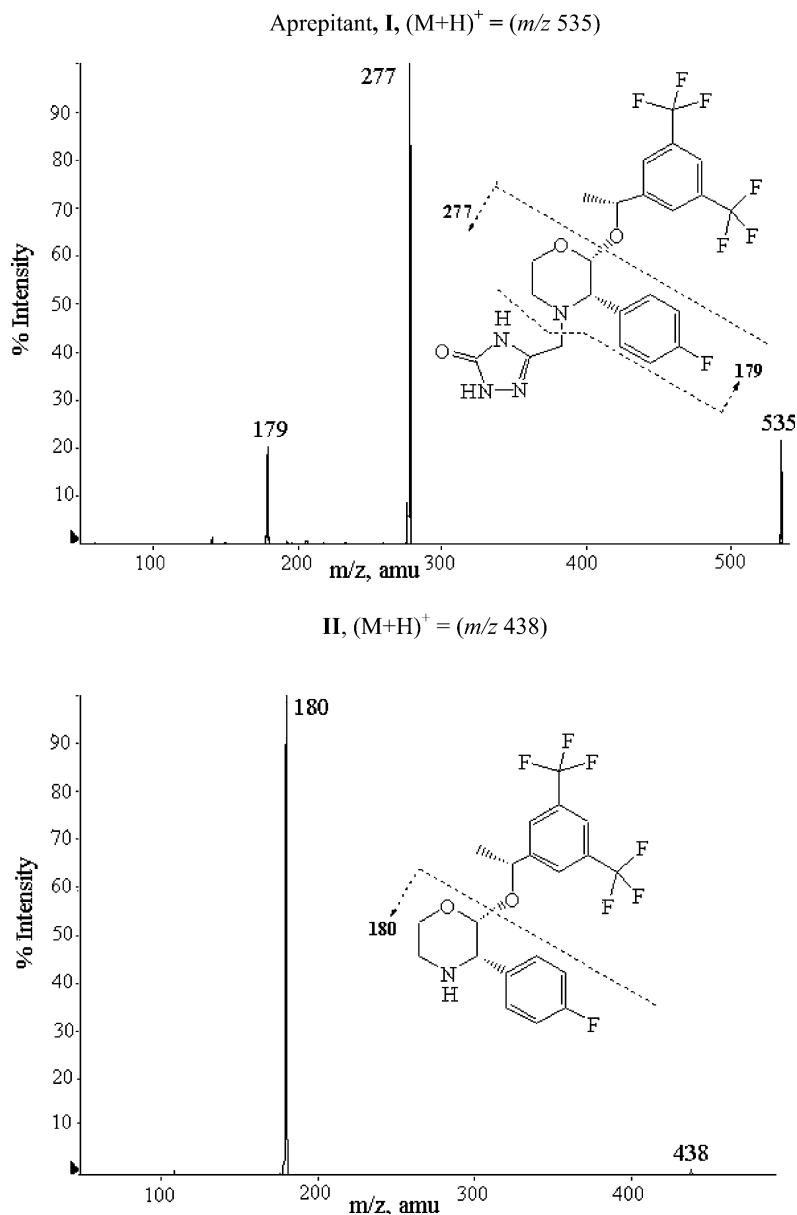
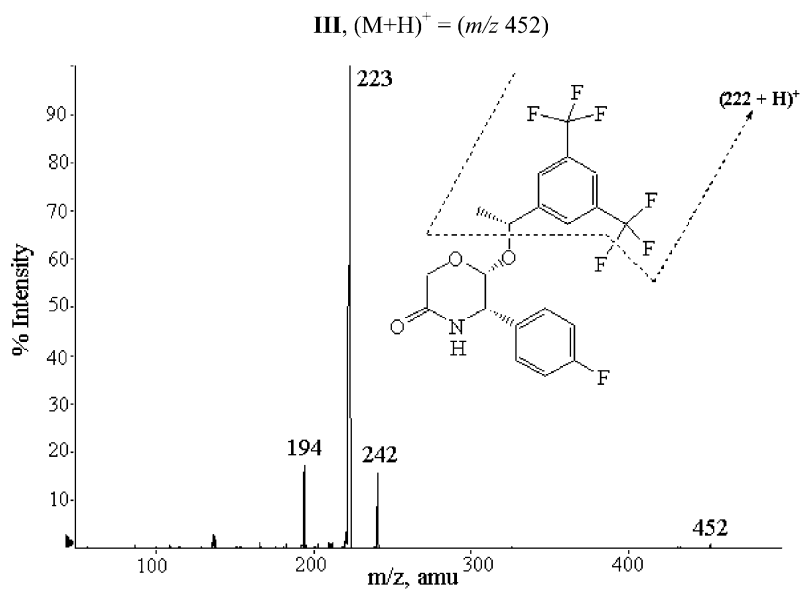


Fig. 2. Positive product ion mass spectra of the protonated molecules of **I**, **II**, **III**, and **IV**.



Internal Standard, **IV, (M+H)⁺ = (m/z 503)**

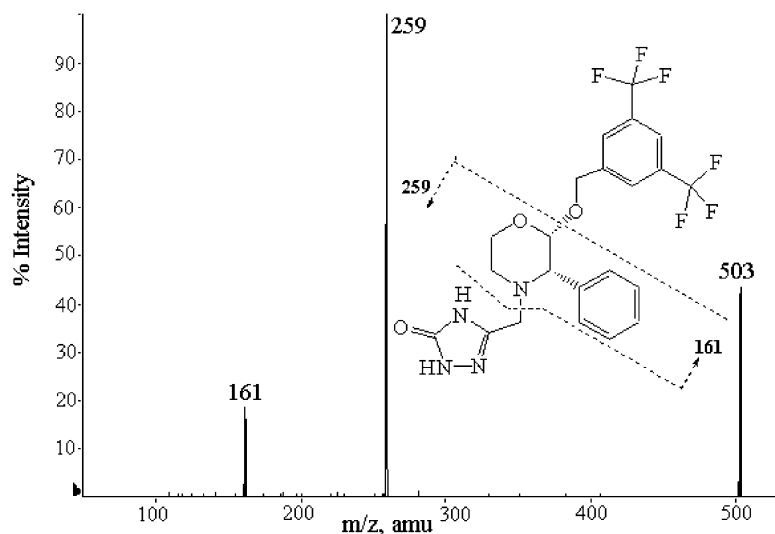


Fig. 2. (Continued).

m/z 535, 438, 452, and 503, respectively. The product ion mass spectra of these protonated molecules (Fig. 2) indicated the presence of intense product ions at *m/z* 277, 180, 223, and 259 for **I**, **II**, **III**, and **IV**, respectively.

The isolation of analytes **I**, **II**, and **III** was based on a liquid–liquid extraction from plasma, evaporation

of the extract to dryness, reconstitution of the residue, and injection of the sample into the HPLC system.

The simultaneous assay for the three analytes was validated in human plasma in the concentration ranges of 10–5000 ng/ml for **I** and **II**, and 25–5000 ng/ml for **III**. The differences between the nominal standard concentrations and the back-calculated concentrations

from the weighted linear regression lines were less than or equal to 5% for each point on the standard curves indicating that the linear regression analysis applied ($1/x^2$) provided an adequate fit of the data. Typical equations for the calibration curves for **I**, **II**, and **III** were $y = 0.004352 \times -0.001856$, $y = 0.002292 \times -0.003648$, and $y = 0.000076 \times -0.000211$, respectively. The correlation coefficients for the mean standard curves obtained in five different plasma lots (set 1) were greater than 0.999 for each of the three analytes, demonstrating linearity over the entire standard curve ranges.

The intra-day accuracy values ranged from 99 to 102, 96 to 102, and 102 to 105% with precision values of less or equal to 2.3, 3.2, 8.5% for **I**, **II**, and **III**, respectively, indicating excellent accuracy and precision of the assay. The assay intra-day accuracy and precision data for the three analytes are summarized in Table 1.

3.2. Assay selectivity

The HPLC-MS/MS conditions used for the determination of **I** [10] were initially utilized during the method development for the simultaneous determination of **I** and two metabolites **II** and **III**. The analytical column in that method was a Keystone Scientific's BDS Hypersil C8 (50 mm \times 4.6 mm, 3 μ m particle size) and the mobile phase was a 50/50 (v/v) mixture of acetonitrile and water containing 0.1% formic acid

and 10 mM ammonium acetate, pumped at 1.0 ml/min. The "cross-talk" between MS/MS channels used for monitoring **I–IV** was evaluated by separately injecting each analyte at the highest concentration on the standard curve and monitoring the responses in the acquisition channels for all analytes. Under the original assay conditions, the retention times of **I**, **II**, **III**, and **IV** were 3.6, 3.8, 5.8, and 3.2 min, respectively. Injection of 100 ng neat standard of **I** on column showed intense responses at the channels corresponding to **I** (m/z 535 \rightarrow 277) and **II** (m/z 438 \rightarrow 180) at the retention time of **I** (3.6 min). Injection of 100 ng neat standard of **II** showed intense response at the channel corresponding to **II** (m/z 438 \rightarrow 180) at a retention time of 3.8 min, but no responses at any other channels. Injecting the same amounts of **III** and **IV** showed intense responses at their respective channels but no responses at any other channels monitored. These results clearly indicated that "cross-talk" existed between MS/MS channels used for monitoring **I** and **II** and baseline separation of these two compounds was required to assure assay selectivity. The "cross-talk" contribution of **I** to the channel used for monitoring **II** may have been due to the in-source fragmentation of **I–II** at the mass spectrometer's interface. For the internal standard (**IV**), the "cross-talk" contribution to the analytes' channels, and vice versa was not observed. Quantification of **I** and **II** under the chromatographic conditions utilized in [10] would not be selective. In addition, the absence of

Table 1

Intra-day precision and accuracy of replicate analysis ($n = 5$) of Aprepitant (**I**), and metabolites (**II**, and **III**) in five different lots of human control plasma

Nominal concentration (ng/ml)	Mean ^a			Precision ^b			Accuracy ^c		
	I	II	III	I	II	III	I	II	III
10	10	10	–	2.1	3.2	–	100	102	–
25	25	24	25	1.7	2.3	8.5	100	96	102
50	50	49	53	2.3	1.2	2.0	101	98	105
100	102	98	104	0.5	1.2	4.5	102	98	104
500	505	505	511	1.8	2.2	3.0	101	101	102
1000	1006	1024	1021	1.1	0.8	1.4	101	102	102
2500	2466	2538	2549	1.5	1.2	2.0	99	102	102
5000	4926	5025	5098	1.8	2.5	1.3	99	100	102

^a Mean concentrations calculated from the weighted linear least-squares regression curve constructed using all five replicate values at each concentration.

^b Expressed as coefficient of variation (CV%).

^c Expressed as [(mean observed concentrations)/(nominal concentration)] \times 100; ($n = 5$).

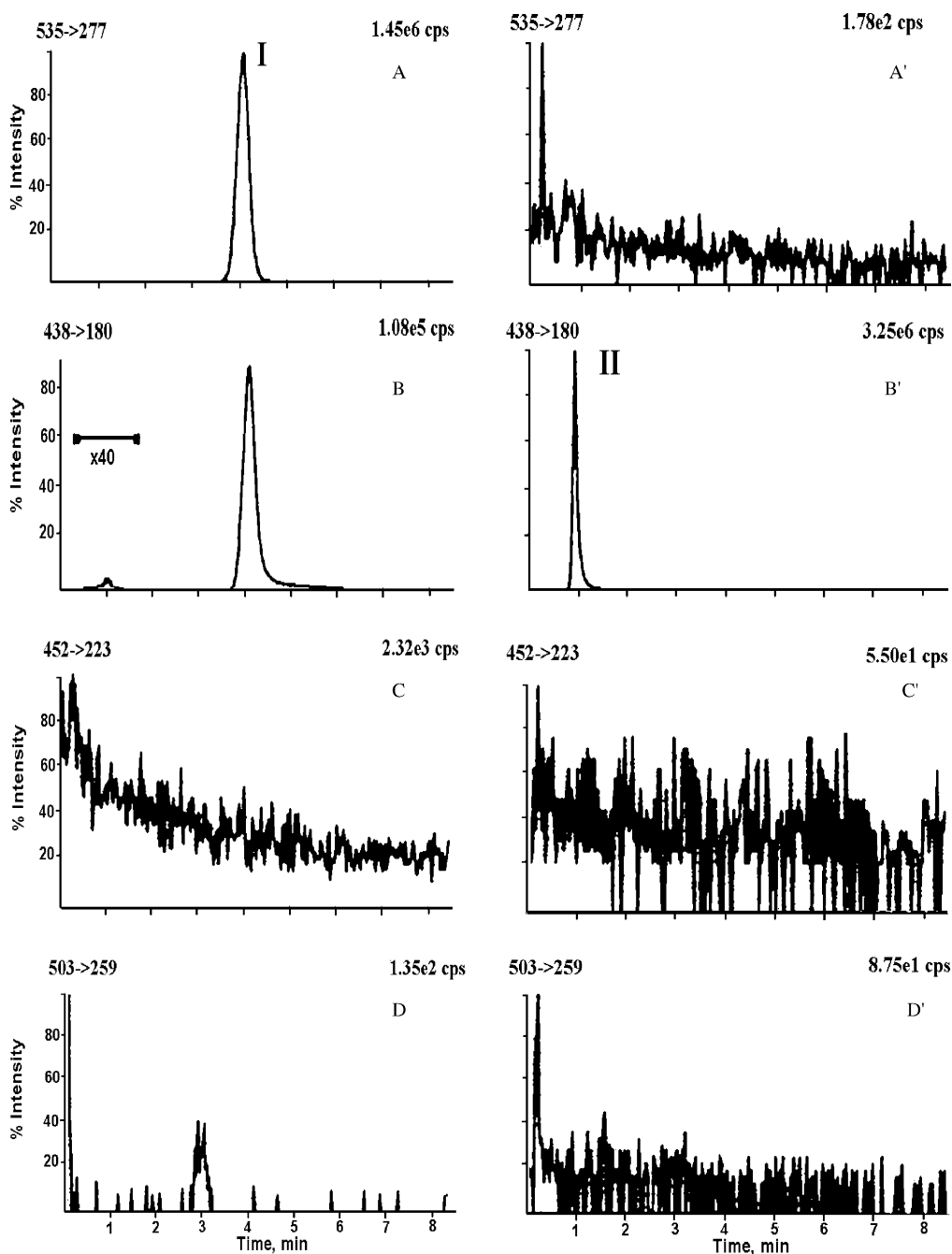


Fig. 3. Representative chromatograms of **I**, **II**, **III**, and **IV** of neat standards monitored at m/z 535 \rightarrow 277 (channel “a”), m/z 438 \rightarrow 180 (channel “b”), m/z 452 \rightarrow 223 (channel “c”), and m/z 503 \rightarrow 259 (channel “d”), respectively. Chromatograms A, B, C, and D are 100 ng neat standard of **I** on column monitored at channels “a”, “b”, “c”, and “d”, respectively; chromatograms A’, B’, C’, and D’—100 ng neat standard of **II** on column monitored at channels “a”, “b”, “c”, and “d”, respectively; chromatograms A’’, B’’, C’’, and D’’—100 ng neat standard of **III** on column monitored at channels “a”, “b”, “c”, and “d”, respectively; chromatograms A’’’, B’’’, C’’’, and D’’’—100 ng neat standard of **IV** on column monitored at channels “a”, “b”, “c”, and “d”, respectively.

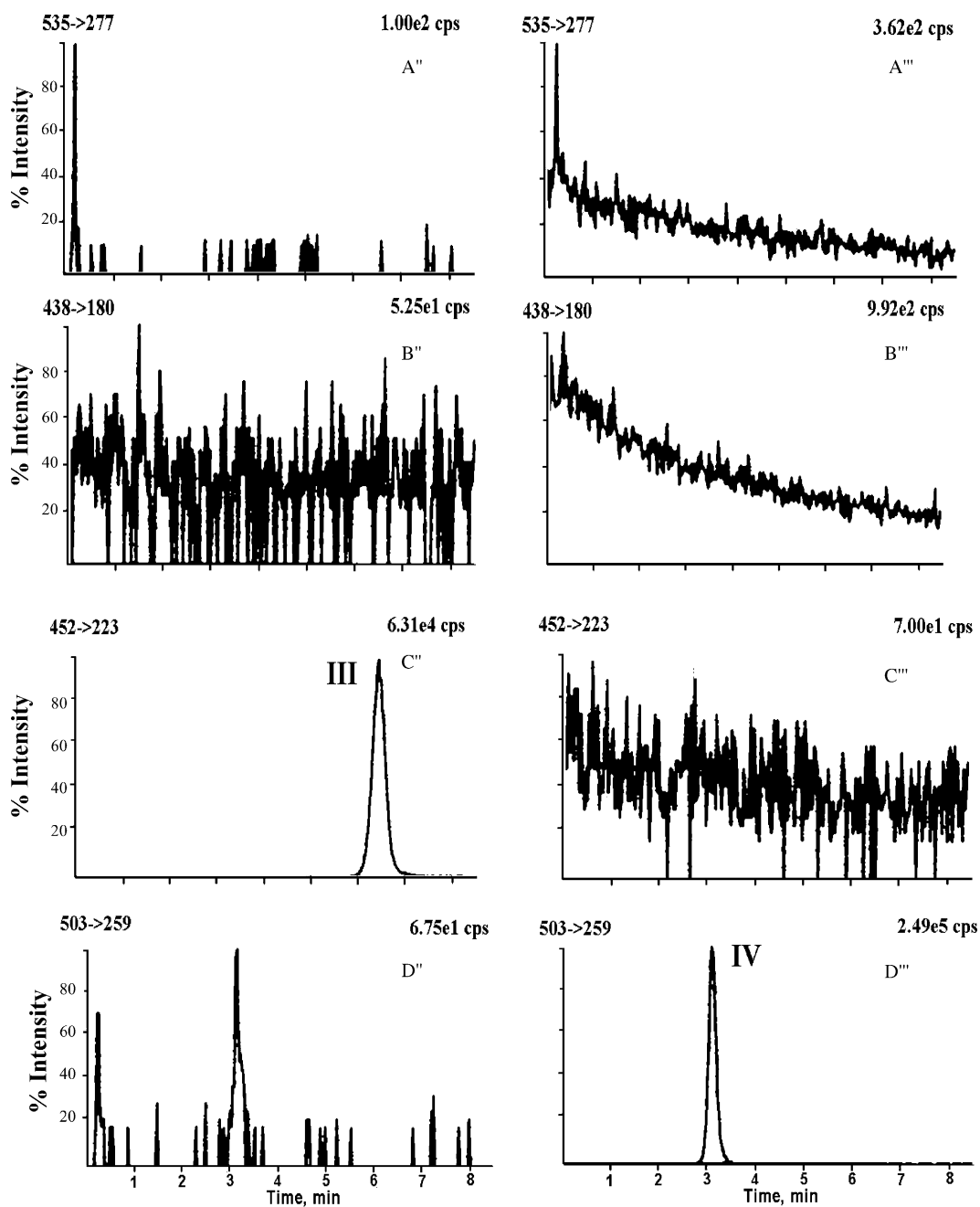


Fig. 3. (Continued).

matrix effect for all analytes and the IS needed to be demonstrated. Therefore, there was a need to design new chromatographic conditions to baseline separate I and II and all other analytes monitored in the

simultaneous assay. Also, by improving separation and retention of analytes on column, the likelihood of elimination of matrix effect for all analytes increases considerably, as demonstrated by us earlier

for other analytes determined by HPLC-MS/MS [11,12].

Different analytical columns (stationary phases) and mobile phase combinations were evaluated to provide better separation and retention of all analytes. TFA was added to the mobile phase although it is known to cause ion suppression especially in electrospray ionization (ESI) due to its ion-pairing activity with the analyte ions. However, in this study, atmospheric pressure chemical ionization was used, and the unfavorable effect of TFA on ionization was not observed. The presence of TFA in the mobile phase showed significant advantage over formic acid in providing better chromatographic retention and separation of the analytes. The HPLC conditions described in the Experimental Section resulted in capacity factors, k' of greater than 4 for all analytes and in the case of **I** and **II** they were 20 and 4, respectively. In addition, good retention of analytes allowed separation of more polar compounds and other potentially interfering compounds from the analytes, thereby potentially decreasing or eliminating the competition for ionization at the retention times of all analytes. However, the good chromatographic retention of analytes ($k' > 4$) on the HPLC column alone may not necessarily guarantee the elimination of matrix effect on quantification and the absence of matrix effect needs to be confirmed. The results of experiments confirming the absence of matrix effect for all analytes are presented in Section 3.3 (see below). The chromatograms of neat standards and blank control plasma extract shown in Figs. 3 and 4 confirmed the absence of any interfering compounds

in plasma extracts under the new HPLC conditions utilized. No detectable endogenous peaks were observed in all channels utilized for analytes' quantification.

3.3. Recovery of analytes and assessment of the matrix effect

The adverse consequences of matrix effects on the results of quantitative HPLC-MS/MS analyses have been fully recognized [11–16] and the assessment of matrix effect is becoming an integral part of method development and validation [10,17–21]. For multi-component assays, the assessment of matrix effect is required for all analytes [12] but is rarely performed in methods described in the literature. In the case of quantitative determination of three analytes described in this paper, the matrix effect and the possibility for ionization suppression or enhancement for **I**, **II**, and **III** in different plasma samples (lots, subjects) under the new HPLC separation conditions were closely examined. The coefficients of variation (CV's, %) of the mean peak areas of **I**, **II**, and **III** (set 1) at any given concentration in five different plasma lots (Table 2) were small (<9%), strongly indicating little or no difference in ionization efficiency and consistent recovery of the analytes from different plasma lots. In addition, by comparing peak areas of all analytes for samples spiked *after* extraction from plasma (Curve 2) with the analogous peak areas obtained by injecting neat standards directly (Curve 1), the extent of the absolute matrix effect was estimated (Table 3). The values >100% indicate ionization enhancement in

Table 2

Mean^a peak areas of **I**, **II**, **III**, and **IV** spiked into five different lots of human plasma before extraction (set 1) and the precision of determination of peak area ratios of analytes (**I**, **II**, or **III**) to the internal standard (**IV**)

Nominal concentration (ng/ml)	Peak area ^b				Peak area ratios ^b		
	I	II	III	IV	I/IV	II/IV	III/IV
10	28045 (2.2)	22429 (0.9)		657547 (2.6)	0.0426 (2.1)	0.0341 (3.2)	
25	67944 (3.0)	54101 (2.6)	3084 (7.2)	653508 (1.9)	0.1039 (1.7)	0.0828 (2.3)	0.0047 (8.5)
50	134300 (2.2)	111071 (2.0)	6499 (3.7)	649595 (1.7)	0.2068 (2.3)	0.1710 (1.2)	0.0100 (2.0)
100	267171 (2.4)	221008 (2.5)	12837 (4.0)	643972 (2.1)	0.4149 (0.5)	0.3432 (1.2)	0.0199 (4.5)
500	1328159 (2.6)	1149379 (1.0)	64041 (1.2)	648674 (2.9)	2.0479 (1.8)	1.7728 (2.2)	0.0988 (3.0)
1000	2616656 (3.1)	2304327 (1.9)	126822 (2.4)	641477 (2.1)	4.0785 (1.1)	3.5924 (0.8)	0.1977 (1.4)
2500	6593654 (2.8)	5872454 (2.3)	325526 (2.2)	659340 (2.5)	10.0007 (1.5)	8.9074 (1.2)	0.4938 (2.0)
5000	13023870 (3.3)	11497587 (1.6)	644068 (2.8)	652064 (2.4)	19.9712 (1.8)	17.6393 (2.5)	0.9877 (1.3)

^a $n = 5$.

^b Numbers in parentheses are coefficient of variation (CV%).

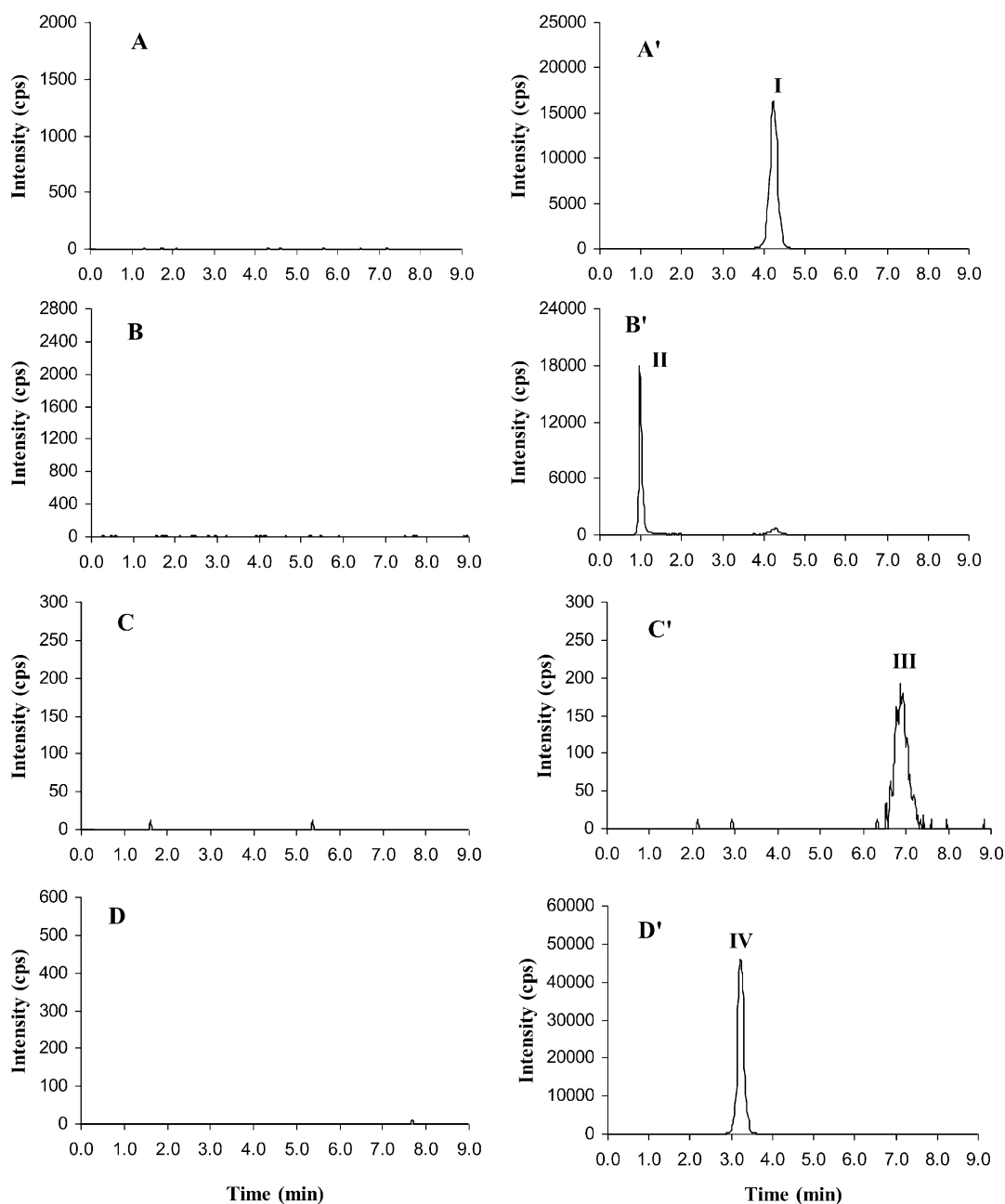


Fig. 4. Representative chromatograms of **I**, **II**, **III**, and **IV** spiked into plasma and monitored at m/z 535 \rightarrow 277 (channel “a”), m/z 438 \rightarrow 180 (channel “b”), m/z 452 \rightarrow 223 (channel “c”), and m/z 503 \rightarrow 259 (channel “d”), respectively. Chromatograms A, B, C, and D are blank control plasma monitored at channels “a”, “b”, “c”, and “d”, respectively; chromatograms A’, B’, C’, and D’—control plasma spiked with 100 ng/ml of **I**, **II**, and **III** and 250 ng/ml of **IV** monitored at channels “a”, “b”, “c”, and “d”, respectively; chromatograms A”, B”, C”, and D”—pooled male predose plasma sample spiked with 250 ng/ml of **IV** monitored at channels “a”, “b”, “c”, and “d”, respectively; chromatograms A”, B”, C”, and D”—pooled male plasma samples Day 4 of 28 days of multiple dosing at 125 mg oral dose, spiked with 250 ng/ml of **IV** monitored at channels “a”, “b”, “c”, and “d”, respectively. Calculated concentrations of **I**, **II**, and **III** were 1393, 70, and 90 ng/ml, respectively.

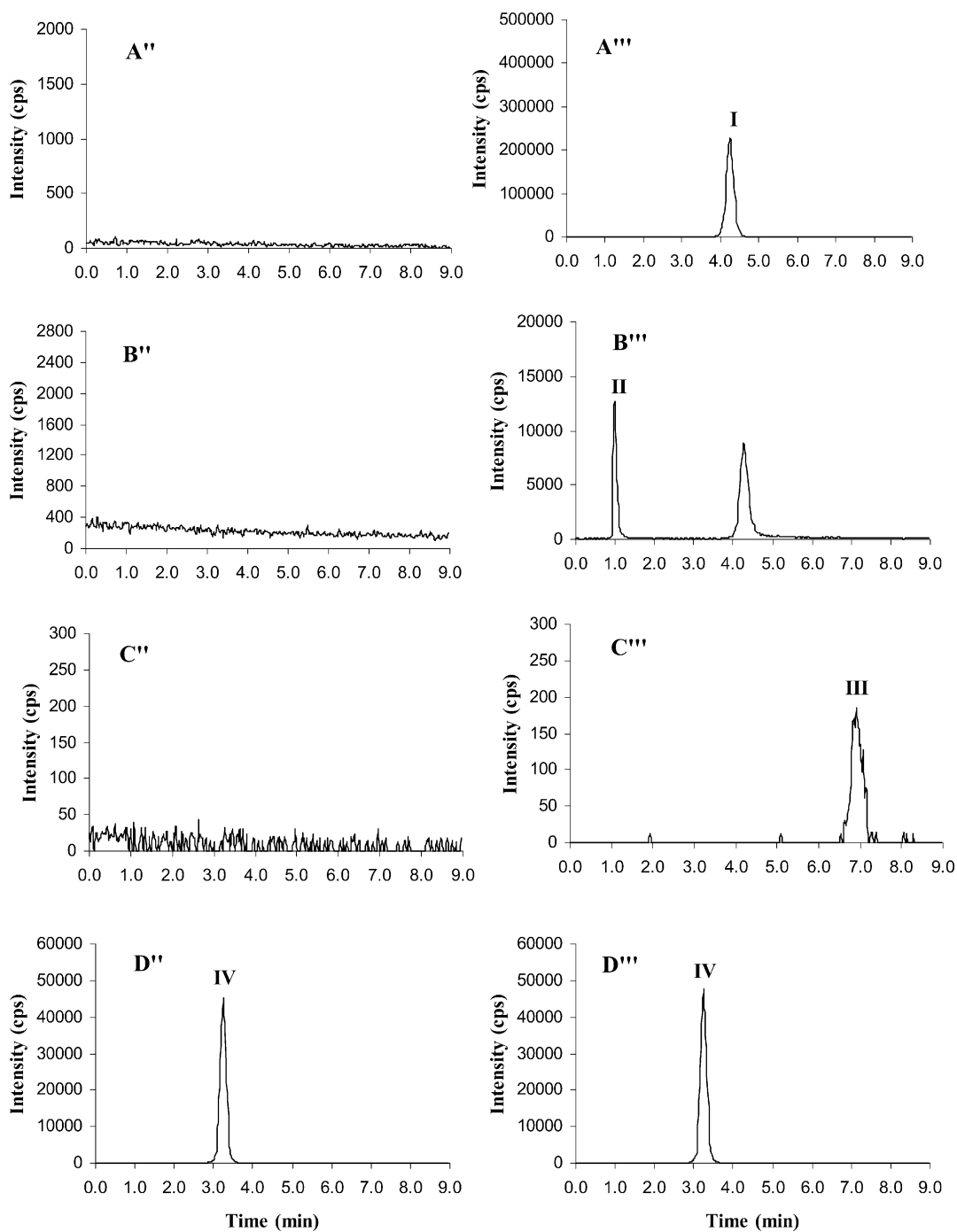


Fig. 4. (Continued).

Table 3
Peak areas of neat standards of **I**, **II**, **III**, and **IV** (Curve 1) and the same standards spiked into plasma *after* extraction (Curve 2)

Nominal concentration (ng/ml)	I			II			III			IV		
	Peak area ^a (A)	Peak area ^b (A')	Matrix effect ^c (A'/A × 100)	Peak area ^a (B)	Peak area ^b (B')	Matrix effect ^c (B'/B × 100)	Peak area ^a (C)	Peak area ^b (C')	Matrix effect ^c (C'/C × 100)	Peak area ^a (D)	Peak area ^b (D')	Matrix effect ^c (D'/D × 100)
10	28309	29678	105	23387	22444	96				692811	685967	99
25	71795	71631	100	61910	57598	93	2999	2873	96	691265	678430	98
50	140624	140839	100	119053	120524	101	6017	6152	102	691294	689080	100
100	277442	280835	101	243784	241258	99	11423	13208	116	671057	704062	105
500	1400383	1384439	99	1189921	1206690	101	59328	61007	103	693178	678960	98
1000	2831494	2770380	98	2437443	2422965	99	124981	127802	102	684871	690260	101
2500	6912717	6906891	100	6145245	6011967	98	307555	322286	105	676282	703882	104
5000	13689260	13971649	102	11648599	12206604	105	630075	642648	102	699467	699887	100
Mean			101			99			104			101
S.D. ^d			2.1			3.6			6.1			2.6
CV% ^e			2.1			3.6			5.9			2.6

^a Neat standards—standard Curve 1 (see Section 2.6).

^b Standards spiked after extraction—standard Curve 2 (see Section 2.6).

^c Matrix effect (%)—expressed as the ratio of the area of an analyte spiked into plasma post-extraction (**A'**, **B'**, **C'**, and **D'**) to the peak areas of the same analyte standards (**A**, **B**, **C**, and **D**) multiplied by 100. A value >100% indicates ionization enhancement, and a value <100% indicates ionization suppression.

^d Standard deviation.

^e Coefficient of variation.

Table 4
Representative standard curve slopes for **I**, **II**, and **III** spiked into five different lots of control human plasma

Calibration curve	Slopes		
	I	II	III
1	0.004054	0.003477	0.000195
2	0.004079	0.003491	0.000198
3	0.004071	0.003495	0.000200
4	0.004071	0.003534	0.000201
5	0.004034	0.003565	0.000200
Mean	0.004062	0.003512	0.000199
Standard deviation	0.000018	0.000036	0.000002
CV% ^a	0.44	1.03	1.01

^a Coefficient of variation.

plasma versus neat standards, whereas values <100% indicate ionization suppression. The data presented in Table 3 indicated that the mean “absolute” matrix effect for **I**, **II**, **III**, and **IV** (101, 99, 104, and 101%, respectively), was negligible.

More importantly, the “relative” matrix effect, based on slopes of the standard curves in different plasma lots (Table 4) was not observed as indicated by a very small coefficient of variation ($\leq 1\%$) of the slopes of standard curves constructed in five different sources of plasma.

The extraction recovery (%) was calculated by comparing the areas of analytes spiked before extraction (set 1) divided by the areas of analytes spiked after extraction (Curve 2) and multiplied by 100. The mean recoveries of **I**, **II**, **III**, and **IV** were 95, 95, 102, and 94%, respectively.

3.4. Freeze–thaw stability

Freeze–thaw stability was examined by exposing quality controls samples to three freeze–thaw cycles (freezer nominal temperature of -20°C). By comparing the initial mean values at three different concentrations of QC standards after one freeze–thaw cycle to the similar mean values after subsequent

Table 5
Analysis of plasma quality control samples for Aprepitant (**I**), **II**, and **III** concentrations

Nominal concentration	LQC ^a concentration (ng/ml)			MQC ^b concentration (ng/ml)			HQC ^c concentration (ng/ml)		
	100			1500			4000		
	I	II	III	I	II	III	I	II	III
Initial mean assayed concentration ^d	102	107	110	1474	1622	4517	3912	1622	4524
S.D. ^e ($n = 5$)	3.1	4.1	4.0	18.6	22.6	59.6	41.5	27.4	89.8
CV ^f (%)	3.0	3.8	3.7	1.3	1.4	1.3	1.1	1.7	2.0
Second Freeze–thaw cycle	102	107	102	1476	1636	4595	3997	1672	4956
S.D. ^e ($n = 2$)	0.9	2.1	0.3	26.2	27.3	120.6	107.2	46.8	350.7
CV ^f (%)	0.9	2.0	0.3	1.8	1.7	2.6	2.7	2.8	7.1
Third Freeze–thaw cycle	105	111	109	1471	1624	4515	3840	1662	4547
SD ^e ($n = 2$)	0.42	0.21	2.8	4.5	24.8	60.0	8.8	23.0	109.7
CV ^f (%)	0.4	0.2	2.6	0.3	1.5	1.3	0.2	1.4	2.4
Inter-day variability ^g overall mean	108	105	115	1540	1612	4395	3972	1564	3953
S.D. ^e	5.8	10.7	8.9	71.4	175.8	389.5	31.3	144.0	455.9
CV ^f (%)	5.4	10.2	7.7	4.6	10.9	8.9	0.8	9.2	11.5
Accuracy ^h (%)	106	98	104	104	99	97	101	96	87

^a Low quality control.

^b Middle quality control.

^c High quality control.

^d Mean of $n = 5$.

^e Standard deviation.

^f Coefficient of variation.

^g Period of 2 days.

^h Accuracy was determined as [(mean determined concentration)/(initial mean assayed concentration)] \times 100.

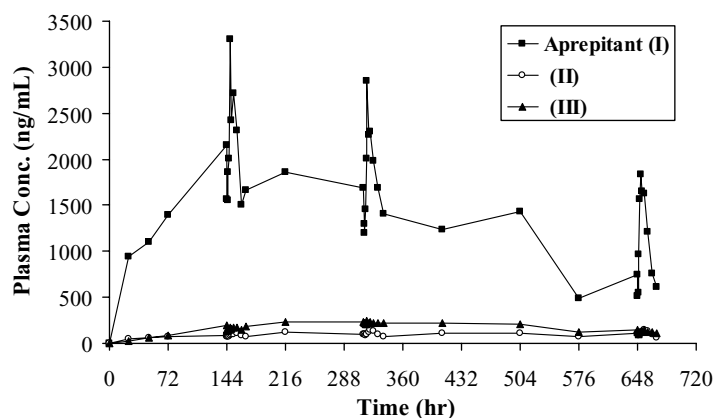


Fig. 5. Pooled ($N = 4$) plasma concentrations of Aprepitant (I), II, and III following multiple 125 mg oral doses of Aprepitant.

freeze–thaw cycles, the effect of freeze–thawing on the stability of all analytes in plasma was determined. There were no significant differences (<4% for I and II; <10% for III) in the assay concentrations following multiple freeze–thaw cycles (Table 5), thus indicating analyte/sample stability. The summary results of the analyses of QC standards during the assay of samples from a clinical trial are presented in Table 5. These data show good inter-assay accuracy and precision of the method for all three analytes.

3.5. Analyses of samples from clinical studies

The simultaneous assay for I and its two metabolites was used to determine the relative concentrations of I, II, and III in pooled human plasma samples. The linear range of the assay (10–5000 ng/ml of plasma for I and II and 25–5000 ng/ml for III) was sufficient to completely map the pharmacokinetic time-profile following the 125 mg oral dose of I. The concentrations of I from pooled plasma samples of male subjects that received daily oral 125 mg dose of I for 28 days ranged from ~616 to 3300 ng/ml while the concentrations of II and III ranged from ~44 to 142 ng/ml, and ~28 to 239 ng/ml, respectively. Based on the binding affinities and concentrations of II and III in plasma, the contribution from metabolites to antiemetic activity of I may be considered as minor. Representative chromatograms of plasma extracts of standards spiked in control plasma and subjects' samples are shown in Fig. 4. Plasma concentrations of I, II, and III ($n = 4$)

following multiple 125 mg capsule doses of I are presented in Fig. 5.

4. Conclusions

The analytical method for the simultaneous determination of Aprepitant (I) and two metabolites (II and III) in plasma, based on liquid–liquid extraction of analytes from basified biological matrix, was developed and validated. The limit of reliable quantification of I and II was 10 ng/ml, and 25 ng/ml for III when 1 ml of plasma was processed. The paper demonstrates the necessity for the careful evaluation of the assay selectivity when multiple analytes are quantified. The absence of matrix effect was demonstrated by analysis of neat standards and standards spiked into plasma extracts originating from five different sources.

Acknowledgements

We would like to thank Drs. R.A. Blum, M.R. Goldberg, and A. Majumdar for their efforts in designing and monitoring the clinical trials with I from which plasma samples for analyses were available.

References

- [1] S. Poli-Bigelli, J. Rodrigues-Pereira, A.D. Carides, G.J. Ma, K. Eldridge, A. Hipple, J.K. Evans, K.J. Horgan, F. Lawson, *Cancer* 97 (2003) 3090–3098.

- [2] P.J. Hesketh, S. Van Belle, M. Aapro, F.D. Tattersall, R.J. Naylor, R. Hargreaves, A.D. Carides, J.K. Evans, K.J. Horgan, *Eur. J. Cancer* 39 (2003) 1074–1080.
- [3] S.P. Chawla, S.M. Grunberg, R.J. Gralla, P.J. Hesketh, C. Rittenberg, M.E. Elmer, C. Schmidt, A. Taylor, A.D. Carides, J.K. Evans, K.J. Horgan, *Cancer* 97 (2003) 2290–2300.
- [4] D. Campos, J. Rodrigues-Pereira, R.R. Reinhardt, C. Carracedo, S. Poli, C. Vogel, J. Martinez-Cedillo, A. Erazo, J. Wittreich, L.-O. Eriksson, A.D. Carides, B.J. Gertz, *J. Clin. Oncol.* 19 (2001) 1759–1767.
- [5] A.R. Martin, A.D. Carides, J.D. Pearson, K. Horgan, M. Elmer, C. Schmidt, B. Cai, S.P. Chawla, S.M. Grunberg, *Eur. J. Cancer* 39 (2003) 1395–1401.
- [6] S.E. Huskey, B.J. Dean, G.A. Doss, Z. Wang, C.E.C.A. Hop, R. Anari, P.E. Finke, A.J. Robichaud, M. Zhan, B. Wang, J.R. Strauss, P.K. Cunningham, W.P. Feeney, R.B. Franklin, T.A. Baillie, S.H.L. Chiu, *Drug Metab. Dispos.*, in press.
- [7] S.E. Huskey, B.J. Dean, R. Bakhtiar, R. Sanchez, F.D. Tattersall, W. Rycroft, R. Hargreaves, A.P. Watt, G.G. Chicchi, C. Keohane, D.F. Hora, S.H.L. Chiu, *Drug Metab. Dispos.* 31 (2003) 785–791.
- [8] S.W. Huskey, B.J. Dean, R.I. Sanchez, C.C.E.A. Hop, Z. Wang, G. Doss, M. Constanzer, C.M. Chavez-Eng, M. Braun, A. Jones, D. Dean, M. Goldberg, G. Murphy, D. Panebianco, S.H.L. Chiu, T.A. Baillie, A. Majumdar, *Drug Metab. Dispos.*, in press.
- [9] M.V.S. Elife, S.W. Huskey, B. Zhu, *J. Pharm. Biomed. Anal.* 30 (2003) 1431–1440.
- [10] M.L. Constanzer, C.M. Chavez-Eng, J. Dru, W.F. Kline, B.K. Matuszewski, *J. Chromatogr. Biomed. Appl.*, in press.
- [11] B.K. Matuszewski, M.L. Constanzer, C.M. Chavez-Eng, *Anal. Chem.* 70 (1998) 882–889.
- [12] B.K. Matuszewski, M.L. Constanzer, C.M. Chavez-Eng, *Anal. Chem.* 75 (2003) 3019–3030.
- [13] G. Hopfgartner, E. Bougogne, *Mass Spectrom. Rev.* 22 (2003) 195–214.
- [14] J. Schuhmacher, D. Zimmer, F. Tesche, V. Pickard, *Rapid Commun. Mass Spectrom.* 17 (2003) 1950–1957.
- [15] H. Mei, Y. Hsieh, C. Nardo, X. Xu, S. Wang, K. Ng, W. Korfmacher, *Rapid Commun. Mass Spectrom.* 17 (2003) 97–103.
- [16] R. Pascoe, J. Foley, A. Gusev, *Anal. Chem.* 73 (2001) 6014–6023.
- [17] M. Jemal, A. Schuster, D.B. Whigan, *Rapid Commun. Mass Spectrom.* 17 (2003) 1723–1734.
- [18] X.-S. Miao, C. Metcalfe, *Anal. Chem.* 75 (2003) 3731–3738.
- [19] R. Dams, C.M. Murphy, W.E. Lambert, M.A. Huestis, *Rapid Commun. Mass Spectrom.* 17 (2003) 1665–1670.
- [20] E. Razzazi-Fazeli, B. Rabus, B. Cecon, J. Bohm, *J. Chromatogr. A* 968 (2002) 129–142.
- [21] G. Ohlenbusch, C. Zwiener, R.U. Meckenstock, F.H. Frimmel, *J. Chromatogr. A* (2002) 201–207.